Influence of laser parameters on nanoparticle-induced membrane permeabilization

Cuiping Yao
Ministry of Education
Key Laboratory of Biomedical Information Engineering
China
and
Xi'an Jiaotong University
School of Life Science and Technology
Institute of Biomedical Analytical Technology and Instrumentation
Xianning xi Road 28
Xi'an, 710049
China

Xiaochao Qu
Xidian University
School of Electronic Engineering
Life Science Research Center
Xi'an, Shaanxi 710071
China

Zhenxi Zhang
Ministry of Education
Key Laboratory of Biomedical Information Engineering
China
and
Xi'an Jiaotong University
School of Life Science and Technology
Institute of Biomedical Analytical Technology and Instrumentation
Xianning xi Road 28
Xi'an, 710049
China

Gereon Hüttmann
Ramtin Rahmanzadeh
University of Lübeck
Institute of Biomedical Optics
Peter-Monnik-Weg 4
Lübeck, D-23562
Germany

Abstract. Light-absorbing nanoparticles that are heated by short laser pulses can transiently increase membrane permeability. We evaluate the membrane permeability by flow cytometry assaying of propidium iodide and fluorescein isothiocyanate dextran (FITC-D) using different laser sources. The dependence of the transfection efficiency on laser parameters such as pulse duration, irradiant exposure, and irradiation mode is investigated. For nano- and also picosecond irradiation, we show a parameter range where a reliable membrane permeabilization is achieved for 10-kDa FITC-D. Fluorescent labeled antibodies are able to penetrate living cells that are permeabilized using these parameters. More than 50% of the cells are stained positive for a 150-kDa IgG antibody. These results suggest that the laser-induced permeabilization approach constitutes a promising tool for targeted delivery of larger exogenous molecules into living cells. © *2009 Society of Photo-Optical Instrumentation Engineers.* [DOI: 10.1117/1.3253320]

Keywords: photothermal effects; photochemical effects; laser; nanoparticles.

Paper 08364RR received Oct. 9, 2008; revised manuscript received Aug. 6, 2009; accepted for publication Aug. 12, 2009; published online Oct. 27, 2009.

1 Introduction

Light-absorbing micro- and nanoparticles, which are bound to cell membranes and irradiated by lasers, have been proven to create highly localized cell damage. By this method, membranes can be permeabilized[1] and our previous results demonstrated the ability to introduce exogenous molecules into mammalian cells using this technique.[2,3]

The introduction of exogenous materials into cells of multicellular organisms using different techniques has been proven to be a powerful approach for the study of gene function and their regulation in bacterial, fungi, animal, and plant cells. Any efficient method for gene transfer could be of considerable value in the continuing progress of genetic engineering. The most common methods for gene transfer involve either the viral vector method or nonviral physical methods such as electroporation. The former is widely used because of its efficiency; but problems associated with safety and limited targeting characteristics exist.[4] Recently, laser-mediated gene transfection has drawn much attention because it is a noncontact and noncontaminating method.[1,5–8]

Laser irradiation parameters, such as irradiance wavelength and pulse duration, and the nature of the absorbing structure are major factors for targeting cells and tissue.[9] Different kinds of lasers that operate with unique pulse durations targeting specific structures were used to introduce exogenous

Address all correspondence to: Ramtin Rahmanzadeh, University of Lübeck, Institute of Biomedical Optics Peter-Monnik-Weg 4, Lübeck, D-23562 Germany. Tel: 49-451-5004695; Fax: 49-451-5006546; E-mail: rahmanzadeh@bmo.uni-luebeck.de

1083-3668/2009/14(5)/054034/7/$25.00 © 2009 SPIE

molecules into cells. Examples include the following: 20-ns 532-nm Q-switched Nd:YAG laser pulse absorbed by gold nanoparticles,[1] latex microparticles targeted by a 532.5-nm Q-switched Nd:YAG laser,[5] 532-nm Q-switched Nd:YAG pulse laser irradiating a strongly absorbing layer,[6–8,10] femtosecond 800-nm titanium-sapphire pulse laser,[11] and *cw* 488-nm argon laser,[12] which both targeted the cell membrane directly. These different lasers carry out three transfection methods: laser microinjection, laser-induced stress wave, and selective cell targeting with light-absorbing particles.

In previous studies we had shown that a permeability of the cell membrane can be caused by laser irradiation of selectively bound gold nanoparticles. Following irradiation, a relatively small 10-kDalton fluorescent labeled dextran was able to penetrate into cells. By comparing the results from different cell lines, the universality of this approach was confirmed.[2] In the present study, we used different laser sources operating at different pulse durations to evaluate their influence on membrane permeability of the human lymphoma cell lines L-428 and Karpas-299. For the first time also, a delivery of a 150-kDa monoclonal IgG antibody into targeted cells was demonstrated.

2 Materials and Methods

2.1 *Apparatus*

Laser irradiation was performed with two nanosecond Q-switched Nd:YAG lasers and one picosecond mode-locked Nd:YLF laser. Both nanosecond lasers were frequency doubled at 532 nm and gave a stable output with a 10% standard deviation and a bell-shaped intensity distribution. However, the different profile bore with a different maximum energy. The first nanosecond laser (Surelite I, Continuum, California) had an oval-shaped beam diameter of approximately 2.5×3.0 mm according to a surface area of 0.06 cm^2. Either a single pulse or multiple pulses at a frequency of about 10 Hz were used. The second nanosecond laser (Spectron, Laser Rugby, Great Britain) had a TEM_{00} Gaussian beam profile with a diameter of 1.0 mm (irradiated area 0.0078 cm^2) and irradiated the samples with a focused beam, which was scanned over the samples with a pulse frequency of 20 Hz.

The pulses of the mode-locked Nd:YLF picosecond laser (ISL 2001 MPL, Intelligent Laser Systems Incorporated, San Diego, California) had a duration of 35 ps at 527 nm. The laser, which was originally built for ophthalmic laser applications, generates a stable output bearing with a 15% standard deviation in a diameter of about 0.5 mm (irradiated area 0.002 cm^2).

Irradiation was performed in wells with a diameter of 1 mm, which were custom-made in 25×75-mm optical glass slides (Hellma, Müllheim, Germany). Each of the 18 wells took a sample volume of 4.0 μl. For irradiation in scanning mode, one well was irradiated with 180 pulses. Each cell was hit with 100 mJ/cm^2 at the maximum, but also with many pulses less than this, due to overlapping pulses of the Gaussian beam profile.

Permeabilization of the plasma membrane was proved by cellular uptake of fluorescein isothiocyanate dextran (FITC-D, molecular weight of 10,000 Daltons, Molecular Probes, Invitrogen, Carlsbad, California) or the Alexa 488 labeled antibody MIB-1, which was kindly provided by Johannes Gerdes of the Leibniz Research Center Borstel in Germany. Cell death was proved by cellular uptake of propidium iodide (PI). The fluorescence was quantified by a flow cytometer (FACScan, Becton Dickinson, Frankil, Lakes, New Jersey) in which the fluorescence of PI and FITC-D was excited with an argon ion laser emitting at 488 nm. Green fluorescence (for FITC-D) and red fluorescence (for PI) were collected using a 525 ± 5-nm bandpass and 600 ± 5-nm long-pass filters, respectively. The data were processed with WinMDI 2.8 software. A total of 5000 cells were examined in each sample. The results were confirmed by fluorescence microscopy (BH2-RFL-T2, Olympus), and the fluorescence images were recorded using a charge-coupled device (CCD) camera.

2.2 *Cell Preparation*

The Hodgkin's disease cell line[13] L-428 and the human non-Hodgkin lymphoma cell line[14] Karpas-299 were also provided by Johannes Gerdes. The cells were routinely grown in suspension culture in RPMI 1640 medium supplemented with Hepes, L-glutamine and 10% fetal calf serum, antibiotic/antimycotic solution (all PAA Laboratories, Pasching, Austria) in a 37 °C humidified incubator (5% CO_2, 95% air). Cells were spun down at 1400 rpm for five minutes at 20 °C, and then resuspended in phosphate buffered saline (PBS) with a density of 4×10^7 cells/ml. The cell concentration was chosen so that the cells build only 1 to 2 cell layers on the well surface to ensure the same irradiation power to all cells. Immunogold conjugates (that is antibody-gold conjugates), prepared from colloidal gold particles with diameters of 15 and 30 nm (British Biocell International, United Kingdom) and the antibodies BerH2 against CD30[15] and ACT-1 against CD25,[16] were prepared according to the manufacturers protocol and added to the cell suspension. The mixture of cells and conjugates was incubated for 20 min at 37 °C. On incubation of the antibody-gold conjugates with the cells, the conjugates will bind to the cell membranes through a strong antibody-antigen binding. Immediately prior to irradiation, 10-kDa FITC-D (or Alexa 488-labeled antibody) was added to test membrane permeabilization. The mixture of cells, nanoparticles, and FITC-D was then transferred to the 18-well glass slide for irradiation. At least 40 min after irradiation, during which the 18-well slide was kept in an incubator, the cells were washed with PBS and then resuspended in PBS with 1-μg/ml propidium iodide (PI) to assay cell death. Subsequently, the fluorescence of the cells was observed by flow cytometry.

3 Results

Three kinds of lasers with different parameters and different irradiation manners were used to irradiate the lymphoma cell lines Karpas-299 and L-428. Four different types of conjugates were prepared from two differently sized gold nanoparticles (15 and 30 nm) and the two antibodies BerH2 and ACT-1, against CD30 and CD25. Using different irradiation modes and different pulse durations, the influence of these parameters could be separated.

First, cells were irradiated with nanosecond single pulses (Surelite I laser) and nanosecond multipulses in scanning

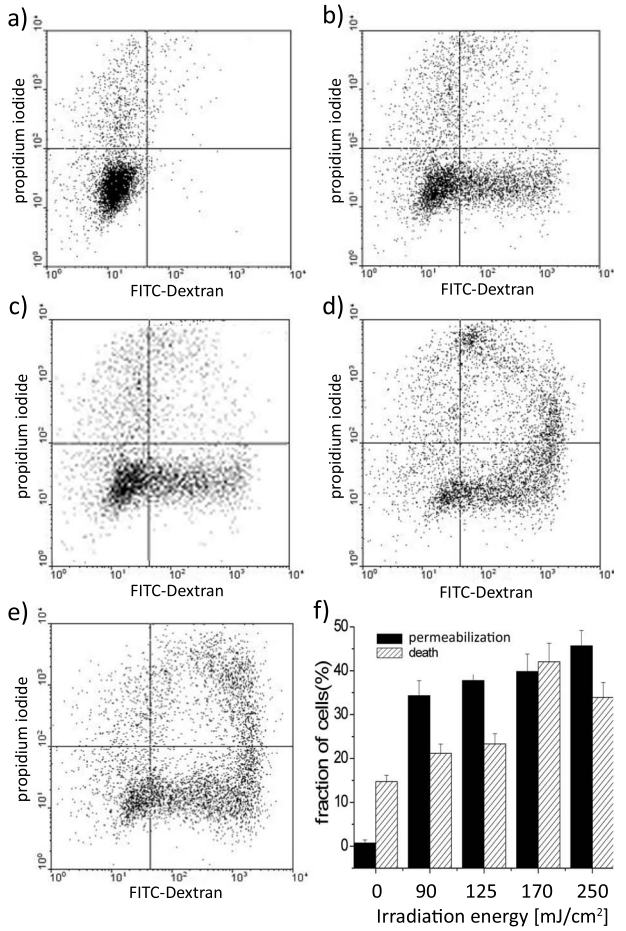

Fig. 1 10-kDa FITC-Dextran uptake by Karpas-299 cells after irradiation with nanosecond single pulses. The cells were incubated with 30-nm ACT-1 immunogold particles and irradiated with different energies: (a) control, no laser; (b) 90 mJ/cm^2; (c) 125 mJ/cm^2; (d) 170 mJ/cm^2; and (e) 250 mJ/cm^2. The percentages of dead (PI positive) and permeabilized cells are given in (f).

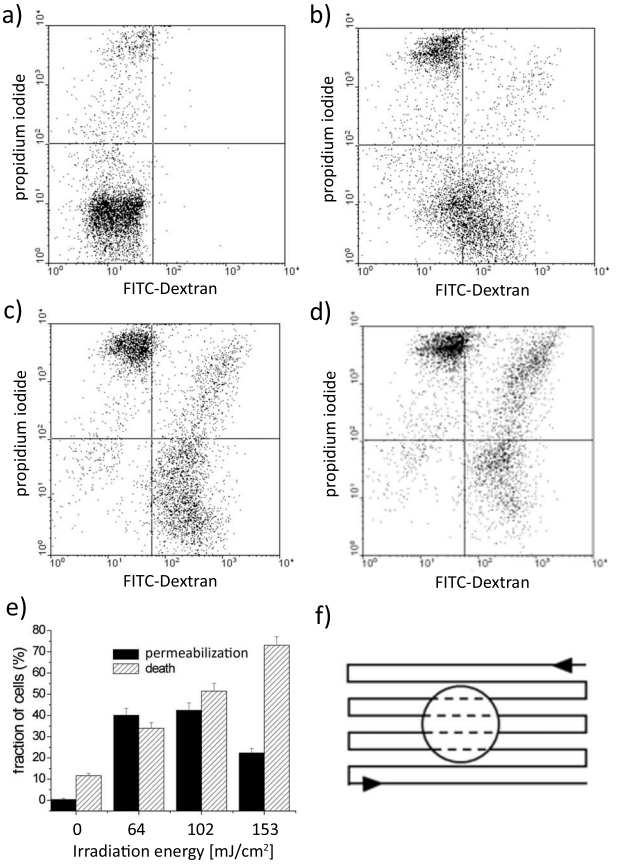

Fig. 2 10-kDa FITC-Dextran uptake by Karpas-299 cells after irradiation with nanosecond pulses in scanning mode. 180 pulses per sample were applied with different energies: (a) control, no laser; (b) 64 mJ/cm^2; (c) 102 mJ/cm^2; and (d) 153 mJ/cm^2. The percentages of dead cells (PI positive) and permeabilized cells are given in (e). A schematic of the scanning pattern is given in (f). One well (circle) was irradiated with 180 overlapping pulses (dashed lines).

mode (Spectron laser). The influence of pulse energy on the permeabilization efficiency was tested on both cell lines with BerH2 and ACT-1 gold conjugates. The results for the Karpas-299 cell line with 30-nm ACT-1 gold conjugates irradiated by single pulses are shown in Fig. 1 and after irradiation with scanning multipulses in Fig. 2. A schematic of the scanning pattern is given in Fig. 2(f). In the dot plots, three subpopulations of cells can be separated: intact viable cells that exhibited no FITC-D and no PI fluorescence (lower left square), transiently permeabilized cells that contained only FITC-D but no PI (lower right square), and permanently damaged or dead cells that were positive for FITC-D and/or PI, which was added at least 40 min after irradiation (upper right square). From the dot plots, a fluorescence threshold for FITC-D was chosen in a way that in the control experiment, less than 5% of cells were positive for FITC-D. The threshold for the PI fluorescence is halfway between the average fluorescence of viable and damaged cells. With these thresholds, the fractions of permeabilized and dead cells were calculated as shown in Figs. 1(f) and 2(e), corresponding to the different pulse energies. Both the fraction of transiently permeabilized cells (lower right square) and the damaged or dead cells (upper right square) increased with increasing pulse energy for both laser sources. Results with the L-428 cell line and 15-nm conjugates are comparable (data not shown), except that the 15-nm particles needed slightly more energy than the 30-nm particles for permeabilization or cell killing.

Both irradiation modes showed comparable results and permeabilization efficiencies between 40 to 50%. The number of permeabilized cells and dead cells both increased with pulse energy and number of applied pulses. More permeabilized cells than dead cells were observed under the appropriate conditions, but when energy and the number of pulses exceeded a certain value, the fraction of permeabilized cells decreased and the fraction of dead cells greatly increased.

To investigate the influences of pulse number for single pulse and scanning mode, the cells were irradiated with the same energy but with differing pulse numbers. For single pulse mode, the samples were irradiated with 10 mJ and 1-to 50 pulses. With increasing number of pulses, the percentage of dead cells increased, whereas the fraction of successfully permeabilized and resealed cells was optimal after 5 pulses and decreased again after irradiation with more pulses [Fig. 3(a)]. For scanning mode, irradiation energy of 100 mJ/cm^2 was used, and pulse numbers were multiples of 180 when a

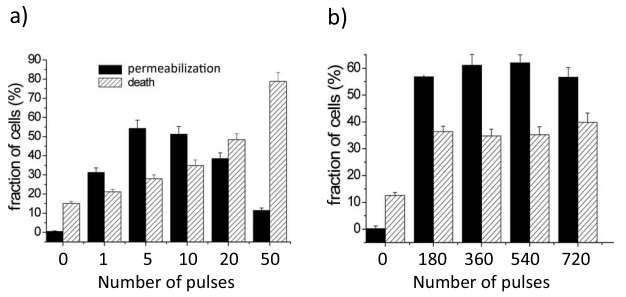

Fig. 3 The percentage of permeabilized and dead cells as a function of pulse number (L-428 cells with BerH2-gold conjugate). (a) Irradiation with nanosecond single pulses of 170 mJ/cm^2. (b) Irradiation with nanoseconds in scanning mode with a maximum pulse energy of 100 mJ/cm^2.

whole well was irradiated fully. Samples were irradiated with 180, 360, 540, and 720 pulses. However, differing from single pulse irradiation, the percentage of the dead cells and the successfully permeabilized cells did not increase with the number of pulses [Fig. 3(b)].

To compare the influence of the different irradiation manners on membrane permeabilization, the results of scanning mode irradiation under optimal conditions are given in Table 1. The permeabilization efficiencies for the different cell lines are in a range from 35 to 65%. For both cell lines, 30-nm conjugates show better transfection results than 15-nm conjugates. These results are very much comparable with the results from single pulse irradiation,[2] with permeabilization efficiencies ranging between 30 and 70%.

To investigate the influence of pulse duration on the transfection efficiency, we compared nanosecond irradiation with the irradiation of a picosecond laser. Both lasers were used for scanning irradiation, and the results are given in Fig. 4. The 30-nm conjugates show better permeabilization results than the 15-nm conjugates when picosecond irradiation is used. The results in L-428 cells with BerH2 gold particles using similar experimental conditions yielded comparable permeabilization rates (data not shown). Based on these results, we conclude that no dramatic dependence on pulse duration exists when the experimental conditions are correctly adjusted for picosecond or nanosecond irradiation.

While the experiments with the dextran served for an optimization of the procedure, the cellular uptake of monoclonal IgG antibodies into cells was investigated as one possible application of a targeted transfer of macromolecules. Karpas-299 cells were incubated with 30-nm Au-BerH2-conjugates, and before irradiation, the Alexa 488 labeled antibody MIB-1 was added. MIB-1 is directed against the nuclear protein Ki-67, which is strongly overexpressed in tumor cells.[17,18] To receive a more distinct separation between surviving and irreversible damaged cells, the PI addition and flow cytometer analysis were performed 12 h after irradiation. With increasing radiant exposure, also the fraction of permeabilized cells increased. The best rate of permeabilization was reached with an irradiance of 90 mJ/cm^2 using a broad nanosecond beam. 50.5% of Karpas-299 cells were positive for MIB-1-Alexa 488 without being permeable for PI. The fraction of permeabilized and PI-positive cells is here 35.5% (Fig. 5)

4 Discussion and Conclusion

Laser-irradiated nanoparticles that are bound to the cell membrane can transiently permeabilize the membrane, allowing macromolecules that normally do not cross the cell membrane to enter the cells. In an earlier study,[2] we could show a transfer of 10-kD dextran by the use of antibody gold conjugates, which were irradiated by a nanosecond pulsed laser. In this work we investigated with different lasers and cell lines the

Table 1 The best efficiencies for scanning mode irradiation for the transfer of 10-kDa FITC-Dextran into Karpas-299 and L-428 cells.

		Conjugate			
Cell	Parameter	BerH2 30 nm	BerH2 15 nm	ACT-1 30 nm	ACT-1 15 nm
Karpas-299	Transfection efficiency	57.06%	47.46%	64.22%	35.6%
	Cell death	22.72%	16.04%	16.12%	19.96%
	Irradiation	0.5 mJ	0.5 mJ	0.5 mJ	0.8 mJ
	Energy and particle load	3.2×10^4/cell	1.1×10^5/cell	4.1×10^4/cell	1×10^5/cell
L-428	Transfection efficiency	53.5%	45.06%		
	Cell death	12.64%	32.54%		
	Irradiation	0.8 mJ	1.2 mJ		
	Energy and particle load	1.44×10^4/cell	3.2×10^5/cell		

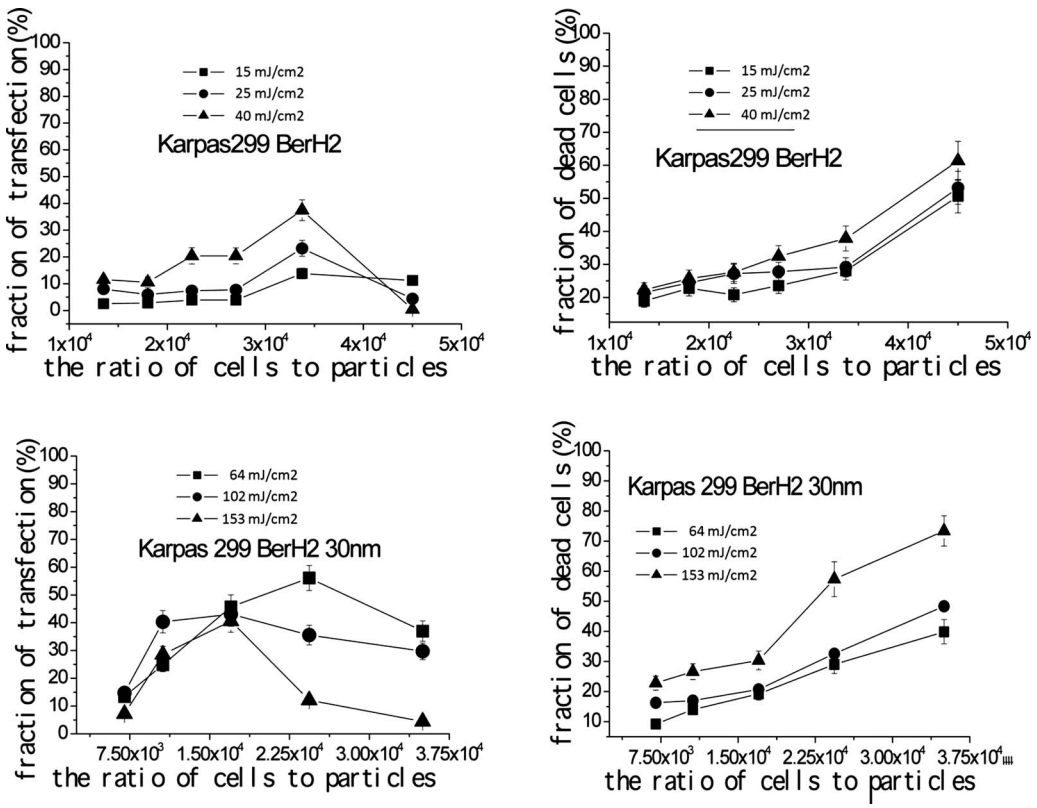

Fig. 4 Influence of pulse duration on membrane permeabilization and cell death for Karpas-299 cells with 30-nm BerH2 gold conjugates. Upper diagrams show irradiation with picosecond pulses with radiant exposure of 15, 25, and 40 mJ/cm^2. Lower diagrams show the results of nanosecond irradiation with 64 mJ/cm^2, 102 mJ/cm^2, and 153 mJ/cm^2. All irradiations are performed in scanning mode.

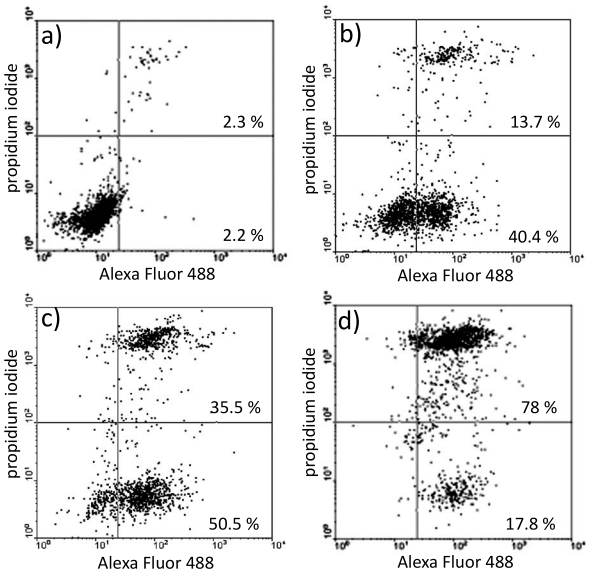

Fig. 5 Cellular uptake of Alexa 488 labeled MIB-1 antibody after single pulse irradiation. Karpas-299 cells were incubated with 30-Au-BerH2-conjugates and irradiated after addition of MIB-1 Alexa 488 with nanosecond single pulses with different energies: (a) control, no laser; (b) 35.4 mJ/cm^2; (c) 53.1 mJ/cm^2; and (d) 88.5 mJ/cm^2. Addition of PI and flow cytometer analysis was performed 12 h after irradiation.

effects of different irradiation modes and pulse durations on transient plasma membrane permeabilization to determine the optimal parameters for a targeted transfer of antibodies into cells.

Our experiments showed that for single pulse irradiation with a broad beam, the membrane permeabilization and death of cells will strongly depend on the number of pulses. After the optimal number of pulses (approximately five), the number of dead cells is increasing and the number of permeabilized cells decreasing. On the other hand, with the scanning mode, once a certain number of pulses occurs, further increase of pulse number will have almost no effect on the cells, even if it is as much as four times the initial quantity. When the same sample was irradiated with different pulses in the scanning mode with a longer interval (e.g., one hour), the dead cells increased and the permeabilized cells decreased dramatically. For nanosecond irradiation, both cell lines incubated with both gold particle diameters in both irradiation modes (single pulse mode or scanning mode) could effectively increase the membrane permeabilization. In comparison, the picosecond laser can also induce membrane permeabilization, but the degree of permeabilization is slightly lower, especially for the 15-nm conjugates.

From all our systemic experimental results, we conclude that all laser parameters, such as pulse duration, irradiation mode, irradiation frequency, and irradiation manner, play important roles in the permeabilization efficiency and death of cells. To determine the corresponding mechanism, it was use-

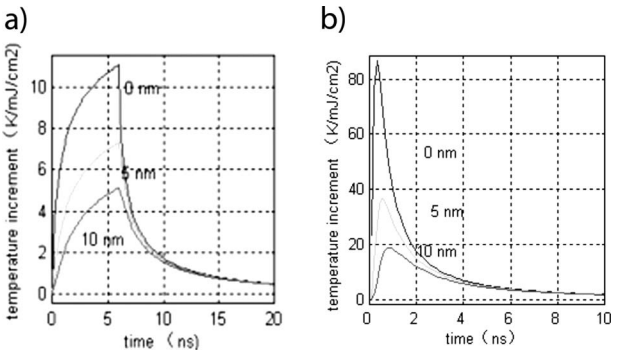

Fig. 6 Temperature change with time at the surface, at 5- and 10-nm distance from the surface, when 30-nm gold particles were irradiated by (a) 6 ns and (b) 35-ps laser pulses with 1 mJ/cm^2.

ful to estimate the magnitude of the transient temperature rise to assess the possibility of the damage.

Estimations of the temperature increase in the particles during irradiation were carried out based on a heat transfer model of a uniformly heated homogeneous sphere embedded in an infinite homogeneous medium developed by Goldenberg and Tranter.[19] For the sake of simplicity, we assumed that the laser intensity was constant during the pulse duration and that the thermal properties of gold and water were independent of temperature.[20,21] The possibility of a phase change in the gold and surrounding water was also not taken into account. The temperature rises and decays at the surface of a 30-nm particle and surrounding water for τ=6 ns and τ=35-ps pulse with 1-mJ/cm^2 radiant exposure are shown in Fig. 6. The temperature increases for nanosecond irradiances that gave good permeabilization results are around 1000 K, whereas picosecond irradiation resulted in two to three times higher temperature increases. Figure 6 a shows the laser-pulse-generated temperature profile, which falls to half its maximum value 10 nm from the gold particle surface. For picosecond irradiation, the heat diffusion is even lower [Fig. 6(b)]; here the temperature profile falls to one quarter of its maximum value at 10-nm distance. These high and localized peak temperatures are necessary for the development of submicrometer cavitation bubbles around the gold nanoparticles. These bubbles are most likely the reason for a mechanical disruption of cell membrane integrity.

Such bubbles with a submicrometer diameter around the gold nanoparticles were experimentally observed under laser irradiation.[22,23] Additionally, the gold melts[24,25] and breaks up into smaller particles. Particle fragmentation was observed at a radiant exposure starting at 80 mJ/cm^2 for 40-nm particles.[26–28] Because the particle temperature is scaled with the square of the particle diameter under nanosecond irradiation, particles below a certain diameter will not reach the melting temperature. Therefore, after a certain number of pulses, no further effect is expected when all particles are fragmented.

Our experiments showed that different laser parameters can be used to transfer comparable small dextrans into the cells. An adjustment of the laser parameters also allowed antibodies that are more than ten times the size of dextran accumulating into the cells. An especially interesting application of a targeted internalization of antibodies is the chromophore-assisted light inactivation (CALI) of proteins.[29] In this approach for functional studies of proteins, irradiated dye antibody conjugates are used to selectively inactivate binding partners of the antibodies. CALI is the only method that gives full temporal and spatial control over the protein inactivation and played for example, a crucial role in functional analysis of the proliferation marker Ki-67.[30] Until now, targeting of proteins inside of cells has been hampered by the difficult and often time-consuming transfer of the dye-conjugates into cells, which is most often done by microinjection. The work presented in this study demonstrates that laser irradiation of nanoparticles shows promise to the automation of CALI.

In summary, we show that after adjustment of different irradiation parameters like irradiation energy and mode, a reliable membrane permeabilization is possible, and we show the use of this method to facilitate entry of antibodies into living cells. The fact that permeabilization is possible with different sized particles, different energies, and with nano- as well as picosecond irradiation will allow the use of many different laser systems. In addition to the previous benefits of this technique, it is possible to target entry of macromolecules into specific cells.

Acknowledgments

We thank Heyke Diddens, Barbara Flucke, Margit Kernbach, and Astrid Rodewald for their help during the experiments. The support of Elmar Endl on flow cytometry is highly appreciated. This work is supported by the China Scholarship Council, the German Ministry for Education and Research (13N8461), National Natural Science Foundation of China (60578026), and the natural Science Basic Project in Shaanxi province, China (Grant No. 2009Q4013).

References

1. C. M. Pitsillides, E. K. Joe, X. Wei, R. R. Anderson, and C. P. Lin, "Selective cell targeting with light-absorbing microparticles and nanoparticles," *Biophys. J.* **84**(6), 4023–4032 (2003).
2. C. Yao, R. Rahmanzadeh, E. Endl, Z. Zhang, J. Gerdes, and G. Hüttmann, "Elevation of plasma membrane permeability by laser irradiation of selectively bound nanoparticles," *J. Biomed. Opt.* **10**(6), 064012 (2005).
3. C. Yao, Z. Zhang, R. Rahmanzadeh, and G. Hüttmann, "Laser-based gene transfection and gene therapy," *IEEE Trans. Nanobiosci.* **7**(2), 111–119 (2008).
4. E. Marshall, "Gene therapy death prompts review of adenovirus vector," *Science* **286**(5448), 2244–2245 (1999).
5. Y. Umebayashi, Y. Miyamoto, M. Wakita, A. Kobaryashi, and T. Nishisaka, "Elevation of plasma membrane permeability on laser irradiation of extracellular latex particles," *J. Biochem. (Tokyo)* **134**(2), 219–224 (2003).
6. M. Terakawa, M. Ogura, S. Sato, H. Wakisaka, H. Ashida, M. Uenoyama, Y. Masaki, and M. Obara, "Gene transfer into mammalian cells by use of a nanosecond pulsed laser-induced stress wave," *Opt. Lett.* **29**(11), 1227–1229 (2004).
7. M. Ogura, S. Sato, K. Nakanishi, M. Uenoyama, T. Kiyozumi, D. Saitoh, T. Ikeda, H. Ashida, and M. Obara, "In vivo targeted gene tranfer in skin by the use of laser-indued stress waves," *Lasers Surg. Med.* **34**(3), 242–248 (2004).
8. Y. Satoh, Y. Kanda, M. Terakawa, M. Obara, K. Mizuno, Y. Watanabe, S. Endo, H. Ooigawa, H. Nawashiro, S. Sato, and K. Takishima, "Targeted DNA transfection into the mouse central nervous system using laser-induced stress waves," *J. Biomed. Opt.* **10**(6), 060501 (2005).
9. M. H. Niemz, *Laser-Tissue Interactions: Fundamentals and Applications*, Springer-Verlag, Berlin (2003).

10. S. Lee, T. Anderson, H. Zhang, T. J. Flotte, and A. G. Doukas, "Alteration of cell membrane by stress waves in vitro," *Ultrasound Med. Biol.* **22**(9), 1285–1293 (1996).
11. U. Tirlapur and K. Konig, "Targeted transfection by femtosecond laser," *Nature (London)* **418**(6895), 290–291 (2002).
12. H. Schneckenburger, A. Hendinger, R. Sailer, W. S. Strauss, and M. Schmitt, "Laser-assisted optoporation of single cells," *J. Biomed. Opt.* **7**(3), 410–416 (2002).
13. M. Schaadt, V. Diehl, H. Stein, C. Fonatsch, and H. H. Kirchner, "Two neoplastic cell lines with unique features derived from Hodgkin's disease," *Int. J. Cancer* **26**(6), 723–731 (1980).
14. P. Fischer, E. Nacheva, D. Y. Mason, P. D. Sherrington, C. Hoyle, F. G. Hayhoe, and A. Karpas, "A Ki-1 (CD30)-positive human cell line (Karpas 299) established from a high-grade non-Hodgkin's lymphoma, showing a 2;5 translocation and rearrangement of the T-cell receptor beta-chain gene," *Blood* **72**(1), 234–240 (1988).
15. R. Schwarting, J. Gerdes, H. Dürkop, B. Falini, S. Pileri, and H. Stein, "Ber-H2: a new anti Ki-1 (CD30) monoclonal antibody directed at s formol-resistant epitope," *Blood* **74**(5), 1678–1689 (1989).
16. R. Schwarting, J. G. J., A. Ziegler, and H. Stein, "Immunoprecipitation of the interleukin-2 receptor from Hodgkin's disease derived cell lines by monoclonal antibodies," *Hematol. Oncol.* **5**(1), 57–64 (1987).
17. G. Key, M. H. Becker, B. Baron, M. Duchrow, C. Schlüter, H. D. Flad, and J. Gerdes, "New Ki-67-equivalent murine monoclonal antibodies (MIB 1-3) generated against bacterially expressed parts of the Ki-67 cDNA containing three 62 base pair repetitive elements encoding for the Ki-67 epitope," *Lab. Invest.* **68**, 629–636 (1993).
18. G. Cattoretti, M. H. Becker, G. Key, M. Duchrow, C. Schlüter, J. Galle, and J. Gerdes, "Monoclonal antibodies against recombinant parts of the Ki-67 antigen (MIB-1 and MIB-3) detect proliferating cells in microwave-processed formalin-fixed paraffin sections," *J. Pathol.* **168**, 357–363 (1992).
19. H. Goldenberg and C. J. Tranter, "Heat flow in an infinite medium heated by a sphere," *Br. J. Appl. Phys.* **3**(9), 296–298 (1952).
20. G. Hüttmann, J. Serbin, B. Radt, B. I. Lange, and R. Birngruber, "Model system for investigating laser-induced subcellular," *Proc. SPIE* **4257**, 398–409 (2001).
21. G. Hüttmann and R. Birngruber, "On the possibility of high-precision photothermal microeffects and the measurement of fast thermal denaturation of proteins," *IEEE J. Sel. Top. Quantum Electron.* **5**(4), 954–962 (1999).
22. V. P. Zharov, V. Galitovsky, and M. Viegas, "Photothermal detection of local thermal effects during selective nanophotothermolysis," *Appl. Phys. Lett.* **83**(24), 4897–4899 (2003).
23. A. Plech, V. Kotaidis, M. Lorenc, and M. Wulff, "Thermal dynamics in laser excited metal nanoparticles," *Chem. Phys. Lett.* **401**(4–6), 565–569 (2005).
24. S. Link, C. Burda, M. B. Mohamed, B. Nikoobakht, and M. A. El-Sayed, "Laser photothermal melting and fragmentation of gold nanorods: energy and laser pulse-width dependence," *J. Phys. Chem. A* **103**(9), 1165–1170 (1999).
25. A. Plech, V. Kotaidis, S. Grésillon, C. Dahmen, and G. v. Plessen, "Laser-induced heating and melting of gold nanoparticles studied by time-resolved x-ray scattering," *Phys. Rev. B* **70**(19), 195423 (2004).
26. H. Kurita, A. Takami, and S. Koda, "Size reduction of gold particles in aqueous solution by pulsed laser irradiation," *Appl. Phys. Lett.* **72**(7), 789–791 (1998).
27. A. Takami, H. Kurita, and S. Koda, "Laser-induced size reduction of noble metal particles," *J. Phys. Chem. B* **103**(3), 1226–1232 (1999).
28. V. Kotaidis and A. Plech, "Cavitation dynamics on the nanoscale," *Appl. Phys. Lett.* **87**(21), 312102 (2005).
29. D. Hoffman-Kim, T. J. Diefenbach, B. K. Eustace, and D. G. Jay, "Chromophore-assisted laser inactivation," *Methods Cell Biol.* **82**, 335–354 (2007).
30. R. Rahmanzadeh, G. Hüttmann, J. Gerdes, and T. Scholzen, "Chromophore-assisted light inactivation (CALI) of pKi-67 leads to inhibition of ribosomal RNA synthesis," *Cell Prolif* **40**, 422–430 (2007).